Cancer Cell
Article

Matuzumab Binding to EGFR Prevents the Conformational Rearrangement Required for Dimerization

Judith Schmiedel,[1,2] Andree Blaukat,[3] Shiqing Li,[1] Thorsten Knöchel,[2,*] and Kathryn M. Ferguson[1,*]
[1]Department of Physiology, University of Pennsylvania School of Medicine, Philadelphia, PA 19104, USA
[2]NCE Lead Discovery Technologies
[3]TA Oncology
Merck Serono Research, Merck KGaA, 64293 Darmstadt, Germany
*Correspondence: ferguso2@mail.med.upenn.edu (K.M.F.), thorsten.knoechel@merck.de (T.K.)
DOI 10.1016/j.ccr.2008.02.019

SUMMARY

An increasing number of therapeutic antibodies targeting tumors that express the epidermal growth factor receptor (EGFR) are in clinical use or late stages of clinical development. Here we investigate the molecular basis for inhibition of EGFR activation by the therapeutic antibody matuzumab (EMD72000). We describe the X-ray crystal structure of the Fab fragment of matuzumab (Fab72000) in complex with isolated domain III from the extracellular region of EGFR. Fab72000 interacts with an epitope on EGFR that is distinct from the ligand-binding region on domain III and from the cetuximab/Erbitux epitope. Matuzumab blocks ligand-induced receptor activation indirectly by sterically preventing the domain rearrangement and local conformational changes that must occur for high-affinity ligand binding and receptor dimerization.

INTRODUCTION

The epidermal growth factor receptor (EGFR) is aberrantly activated in a variety of epithelial tumors and has been the focus of much interest as a target in anticancer therapy. EGFR is one of a family of four receptor tyrosine kinases (collectively known as the ErbB or HER receptors) that are involved in critical cellular processes such as proliferation, differentiation, and apoptosis (Hubbard and Miller, 2007; Schlessinger, 2000). Misregulation of EGFR, through overexpression or mutation, leads to constitutive activity or impaired receptor downregulation and can cause malignant transformation of the cell (Mendelsohn and Baselga, 2006).

Based on structural studies over the past 5 years of the ErbB receptors, a model has been proposed for ligand-dependent dimerization and activation of EGFR (Figure 1) (Burgess et al., 2003; Ferguson et al., 2003; Zhang et al., 2006). Dimerization of the EGFR extracellular region is entirely receptor mediated, with the majority of interactions contributed by domain II of EGFR (Garrett et al., 2002; Ogiso et al., 2002). In the unliganded state, the receptor adopts a very different conformation that occludes much of the domain II dimerization interface in an intramolecular interaction or tether with domain IV (Bouyain et al., 2005; Cho and Leahy, 2002; Ferguson et al., 2003). Upon ligand binding, the extracellular region of EGFR must undergo a dramatic domain rearrangement, which exposes the domain II dimerization interface. Additional localized ligand-induced changes stabilize the precise conformation of domain II that is required for dimerization (Dawson et al., 2005). Receptor dimerization brings the intracellular regions into close proximity, promoting the allosteric activation of the kinase domains (Zhang et al., 2006).

This mechanism suggests a number of ways to inhibit EGFR activation through interaction with the extracellular region of the receptor (Ferguson, 2004). X-ray crystallographic and biochemical analysis of receptor-antibody complexes have indicated several modes of binding that lead to effective inhibition of

SIGNIFICANCE

Antibodies targeting the EGF receptor family are proven anticancer drugs. The anti-ErbB2 antibody trastuzumab/Herceptin is established as a treatment of ErbB2-positive breast cancer, and therapeutic protocols are in clinical use for two EGFR-targeting antibodies, cetuximab/Erbitux and panitumumab/Vectibix. Matuzumab, a humanized form of the mouse anti-EGFR mAb425, is in phase II clinical trials. Our studies show that both the epitope for and the mechanism of inhibition by matuzumab are distinct from those for cetuximab. We show that matuzumab and cetuximab can both simultaneously bind to EGFR, implying that combination therapy with both antibodies could be advantageous. This has important implications for the clinical use of matuzumab and in moving forward with the development of therapeutic approaches targeting the EGF receptor.

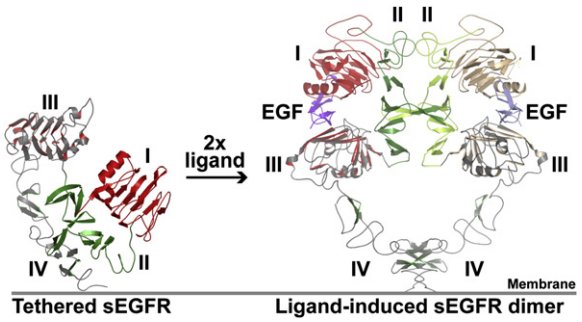

Figure 1. Ligand-Induced EGF Receptor Dimerization

The extracellular region of the EGF receptor (sEGFR) is shown in cartoon representation with domain I in red, domain II in green, and domains III and IV in gray, with the secondary structure elements highlighted in red and green, respectively. The inactive receptor (left-hand view) exists in a tethered, autoinhibited conformation with an intramolecular interaction between domains II and IV. Upon ligand binding, the receptor adopts a very different domain arrangement (right-hand view). Ligand (here EGF, shown in purple cartoon) binds between domains I and III of a single EGFR molecule, stabilizing the precise, extended configuration of EGFR that can dimerize. All contacts between the two molecules in the dimer are receptor mediated, with domain II providing the primary dimerization contacts. EGF receptor dimerization is ligand induced, but entirely receptor mediated. The colors on the right-hand molecule in the sEGFR dimer have been muted for contrast. Coordinates from PDB IDs 1IVO and 1NQL were used to generate this figure. Domain IV in the sEGFR dimer was modeled as previously described (Ferguson et al., 2003).

ErbB receptor signaling. The chimeric antibody cetuximab/Erbitux (Imclone/BMS and Merck KGaA) binds to domain III of EGFR, directly blocking ligand binding (Li et al., 2005). Another anti-EGFR antibody, mAb806, binds to domain II close to the receptor dimerization site (Johns et al., 2004). The anti-ErbB2 antibody pertuzumab/Omnitarg (Genentech) binds to the domain II dimerization arm and prevents ligand-induced ErbB2 heterodimerization (Franklin et al., 2004), while trastuzumab/Herceptin (Genentech) binds to the membrane-proximal domain IV of ErbB2 (Cho et al., 2003) and likely modulates a cleavage event that leads to ectodomain shedding and kinase activation (Molina et al., 2001).

We were interested to establish the mode of inhibition of EGFR by another therapeutic antibody, matuzumab (EMD72000), which targets EGFR-expressing tumors. Matuzumab is the humanized form of the murine mAb 425 (EMD55900) that was produced by immunization of BALB/c mice with human A431 epidermoid carcinoma cells (Kettleborough et al., 1991; Murthy et al., 1987). Monoclonal antibody 425 (EMD55900) blocks ligand-dependent activation of EGFR in tumor cell lines (Rodeck et al., 1990) and has been demonstrated to inhibit growth of EGFR-dependent tumors in preclinical studies (Rodeck et al., 1987). Matuzumab has performed well in phase I clinical trials against a number of cancers, both alone and in combination with chemotherapy (Bier et al., 2001; Graeven et al., 2006; Kollmannsberger et al., 2006; Vanhoefer et al., 2004), and is being actively pursued in multiple ongoing phase II trials (Seiden et al., 2007; Socinski, 2007).

Here we describe the crystal structure of the Fab fragment of matuzumab (Fab72000) bound to a truncated form of the extracellular region of EGFR that comprises all of domain III plus the first 24 amino acids from domain IV. Matuzumab binds to an epitope on domain III of EGFR that is distinct from both the ligand-binding site and the cetuximab epitope on that domain. Matuzumab does not directly block the access of ligand to the domain III-binding site, and thus does not share the primary mechanism for inhibition of ligand-induced EGFR activation employed by cetuximab. Rather, the binding of matuzumab to domain III sterically blocks the domain rearrangement that is required for high-affinity ligand binding and receptor dimerization. Further, binding to this epitope places the antigen-binding domains of matuzumab such as to impede the formation of the critical contacts between domains II and III that are required to stabilize the dimerization competent conformation of domain II. This noncompetitive mechanism of inhibition of EGFR activation has implications for both the application of current drugs and the development of anti-EGFR therapeutics.

RESULTS AND DISCUSSION

Binding Characteristics of Matuzumab to Cell Surface and Soluble EGFR

To determine the mode of binding of matuzumab to EGFR, and to elucidate the mechanism of inhibition of EGFR by this therapeutic antibody, we sought to determine the X-ray crystal structure of the complex between the Fab fragment of the antibody and the extracellular region of EGFR. We first characterized the binding of matuzumab to the soluble extracellular domain of EGFR (sEGFR) and compared the results to the behavior of this antibody in cell surface binding assays.

Soluble EGFR was produced by secretion from baculovirus-infected Sf9 cells and purified exactly as described (Ferguson et al., 2000). The Fab fragment of matuzumab (Fab72000), produced by papain cleavage of the antibody, was immobilized on a CM5 biosensor chip (see Experimental Procedures). Using surface plasmon resonance (SPR/Biacore), we established that sEGFR binds to this immobilized Fab72000 with a K_D value of 113 ± 25 nM (Figure 2A). This value is weaker than that observed for the binding of ^{125}I-labeled intact matuzumab to cell surface EGFR (about 1–10 nM, depending on the cell line employed; data not shown), although these binding assays are not directly comparable. It has previously been shown that the epitope for cetuximab lies exclusively on domain III of sEGFR (Li et al., 2005). To address whether this is also true for matuzumab, we produced and purified isolated domain III of sEGFR (sEGFRd3; amino acids 311–514 of mature EGFR) exactly as described (Li et al., 2005). As shown in Figure 2A, sEGFRd3 binds to immobilized Fab72000 with a K_D value of 43.0 ± 12.9 nM. The antigen-binding domain of matuzumab, like that of cetuximab, binds more tightly to sEGFRd3, possibly due to the absence of steric hindrance from the other domains of sEGFR.

We next used both SPR and cell surface binding analysis to investigate the ability of matuzumab to compete with ligand binding to EGFR. As shown in Figure 2B, matuzumab, like cetuximab, competes efficiently for the binding of 3 nM ^{125}I-labeled EGF to the surface of A431 epidermoid carcinoma cells. It has previously been shown that, in the context of an SPR/Biacore assay, the Fab fragment of cetuximab (FabC225) is able to block all binding of soluble sEGFR to immobilize EGF (Li et al., 2005). We asked if this is also true for the Fab fragment of matuzumab. Samples of 600 nM sEGFR containing increasing excesses of Fab72000 were passed over a biosensor surface to which EGF

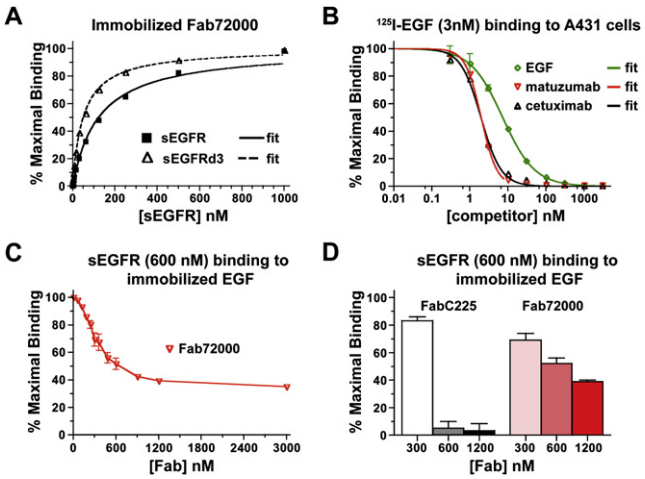

Figure 2. Characterization of the EGFR-Binding and Ligand Competition Properties of Matuzumab

(A) Surface Plasmon Resonance (SPR) analysis of the binding of sEGFR and sEGFRd3 to immobilized Fab72000 (the antigen-binding domain of matuzumab). A series of samples of sEGFR or sEGFRd3, at the indicated concentrations, was passed over a biosensor surface to which Fab72000 had been amine coupled. Data points show the equilibrium SPR response value for a representative set of samples of sEGFR (black squares) and of sEGFRd3 (open triangles), expressed as a percentage of the maximal SPR-binding response. The curves represent the fit of these data to a simple one-site Langmuir binding equation. K_D values, based on at least three independent binding experiments, are 113 ± 25 nM for sEGFR and 43 ± 13 nM for sEGFRd3.

(B) Competition of EGF (green diamonds), matuzumab (red triangles), or cetuximab (black triangles) for the binding of ^{125}I-labeled EGF to A431 cells. Cells were incubated with media containing 3 nM ^{125}I-labeled EGF plus the indicated concentration of cold matuzumab, cetuximab, or EGF for 6 hr at 4°C. Following washing to remove unbound material, cells were lysed and liquid scintillation counting was used to determine the amount of bound ^{125}I-labeled EGF. The counts per minute (CPM) for each sample are shown, expressed as a percentage of the CPM value obtained for no added competitor. Error bars indicate the standard deviation on three independent experiments. The line indicates the fit to a sigmoidal dose-response model. IC_{50} values from this analysis are 2.0 nM for matuzumab and cetuximab and 7.3 nM for EGF.

(C) A competition experiment showing the effect of addition of Fab72000 upon the binding of 600 nM sEGFR to immobilized EGF. Mixtures of 600 nM sEGFR plus the indicated concentrations of Fab72000 were passed over a biosensor surface to which EGF had been amine coupled. The equilibrium SPR responses for each mixture is shown, normalized to the response obtained with no added Fab. Error bars indicate the standard deviation on at least three independent measurements. The line simply connects the data points.

(D) The ability of FabC225 (the antigen-binding domain of cetuximab; gray shades) and Fab72000 (red shades) to compete for the binding of 600 nM sEGFR to immobilized EGF, determined exactly as described in (C). Samples of each Fab alone show no binding to the immobilized EGF (data not shown). Data for FabC225 taken from Li et al. (2005). Error bars indicate the standard deviation on at least three independent measurements.

had been immobilized. As shown in Figure 2C, there is an initial decrease in the equilibrium SPR response as increasing Fab72000 is added. At a 1:1 molar ratio of Fab72000:sEGFR, the SPR response is about 45% of that obtained with no added Fab. Addition of increasing excesses of Fab72000 does not further reduce this binding level. Even at a higher concentration of sEGFR and with up to a 50-fold excess of Fab72000 (data not shown), the equilibrium SPR response does not fall below 40% of the value in the absence of added Fab. One possible explanation for the observed SPR responses in Figure 2C is that both unbound sEGFR and the Fab72000/sEGFR complex can interact with the immobilized EGF, but that the complex binds with substantially weaker affinity. Equilibrium binding analysis to immobilized EGF for samples of sEGFR containing a 10-fold molar excess of Fab72000 indicates an apparent K_D value that is approximately 5-fold weaker than that for sEGFR alone (data not shown). Certainly these data suggest that there must be something quite different about the mode of binding to sEGFR of the Fab fragment of matuzumab compared to that of cetuximab. Both antibodies are able to compete for binding of low concentrations of EGF to cell surface EGFR, yet the Fab fragments from the two antibodies have very different effects on the ability of soluble EGFR to bind to immobilized EGF in the Biacore assay (Figure 2D and Li et al., 2005).

To gain further insight into the precise mode of binding of matuzumab to EGFR, and to understand how this leads to inhibition of cell surface ligand binding and of ligand-stimulated EGFR activation, we crystallized and solved the structures of Fab72000 alone and in complex with the sEGFRd3 (see Experimental Procedures and Table 1).

The Structure of the Fab72000/sEGFRd3 Complex

Crystals of the isolated Fab72000 that diffract to 2.15 Å resolution were obtained, and the structure was solved by molecular replacement (MR) methods using as search model the coordinates of an Fab fragment selected by degree of sequence similarity (Protein Data Bank [PDB] ID 1L7I). A complex of sEGFRd3 and Fab72000 was purified by size exclusion chromatography (SEC), and crystals that diffract to 3.2 Å resolution were obtained using streak seeding techniques. To solve this structure, MR search models based on the coordinates for domain III of sEGFR (PDB ID 1YY9) and the coordinates of the refined Fab72000 were used to locate the two Fab72000/sEGFRd3 complexes in the asymmetric unit. Data collection and refinement statistics are given in Table 1.

Fab72000 binds primarily to the loop that precedes the most C-terminal strand of the domain III β-helix (amino acids 454–464; highlighted in red in Figure 3A). This loop penetrates into a cleft between the V_L and V_H domains of the Fab. The tip of this loop forms a type I beta turn, with T459 and S460 in this turn protruding the farthest into the cleft. This mode of binding is unusual for the recognition of a large protein antigen, where it is more common for the epitope to comprise a large flat surface on the antigen (Sundberg and Mariuzza, 2002), as was observed for the binding of cetuximab to EGFR (Li et al., 2005). All of the key interactions made by the Fab are from the complementarity-determining regions (CDRs), with the major specificity-determining contacts coming from CDRs H3 and L3. All of the CDRs contribute to binding to domain III, also an unusual feature compared to most antigen-antibody complexes (Sundberg and Mariuzza, 2002).

The tip of the buried loop from sEGFR makes interactions with both the heavy- and light-chain CDRs (Figure 3B); the side chain of T459 interacts with that of H93 from the Fab light chain, while the side chain of S460 contacts the CDR H2 side chain E50. Two lysines, one on either end of the sEGFRd3 epitope loop, form salt bridge interactions with aspartic acids on the Fab (K454 with D100 from CDR H3 and K463 with CDR L2 D49). Additional

Table 1. Data Collection and Refinement Statistics

	Fab72000	Fab72000/sEGFRd3
Data Collection Statistics[a]		
Space group	$P2_12_12_1$	C2
Unique cell dimensions	a = 56.8 Å, b = 61.4 Å, c = 102.7 Å	a = 141.1 Å, b = 205.0 Å, c = 81.6 Å, β = 117.5°
X-ray source	CHESS F1	SLS X06SA
Resolution limit	2.15 Å	3.2 Å
Observed/unique	107,297/ 20,191	120,206/33,886
Completeness (%)	99.9 (99.9)	99.7 (98.7)
R_{sym}[b]	0.10 (0.42)	0.12 (0.35)
$\langle I/\sigma \rangle$	20.7 (3.6)	11.4 (3.4)
Refinement Statistics		
Resolution limits	50–2.15 Å	50–3.2 Å
No. of reflections/no. test set	19,098/1029	32,028/1709
R factor (R_{free})[c]	0.22 (0.26)	0.24 (0.29)
Model	one Fab72000 molecule	two Fab72000/sEGFRd3 complexes
Protein	aa 4–211 of light chain; aa 1–224 of heavy chain	aa 310–500 of mature sEGFR with 13 saccharide units; aa 1–211 of Fab light chain; aa 1–135, 142–222 of Fab heavy chain[d]
Water/ions	99 water molecules; 2 sulfates	—
Total number of atoms	3209	8517
RMSD bond length (Å)	0.012	0.015
RMSD bond angles (°)	1.35	1.6

[a] Numbers in parentheses refer to last resolution shell.
[b] $R_{sym} = \Sigma|I_h - \langle I_h \rangle|/\Sigma I_h$, where $\langle I_h \rangle$ is the average intensity over symmetry equivalent measurements.
[c] R factor = $\Sigma||F_o| - |F_c||/\Sigma|F_o|$, where summation is over data used in the refinement; R_{free} includes 5% of the data excluded from the refinement.
[d] Number of missing amino acids in the heavy and light chains differs in the two complexes.

interactions with the buried epitope loop are contributed by side chains in CDRs H1, H2, and L1 that are within hydrogen-bonding distance of the main chain of sEGFRd3 (Figure 3B and Figure S1 available online). Two important direct interactions are made between the Fab and regions of domain III outside the loop between amino acids 454–464. A histidine from CDR L3 (H93) interacts with D434 on the adjacent loop of the sEGFRd3 β-helix, while on the other side of the binding site Y103 from the apex of CDR H3 extends to interact with N449. These two interactions anchor the Fab over the central binding loop and expand the epitope substantially beyond the single peptide loop.

A total of two salt bridges and 11 predicted hydrogen bonds are involved in the interaction between Fab72000 and sEGFRd3, in an interface that buries 758 $Å^2$ of solvent-accessible surface on domain III (a total of 1516 $Å^2$ of surface is occluded from solvent in the complex). The shape complementarity (sc) parameter for the interface of the Fab72000/sEGFRd3 complex is 0.62, slightly lower than is typically observed for antigen-antibody interfaces (0.64 to 0.68) (Lawrence and Colman, 1993). The sc values reported for cetuximab bound to EGFR (Li et al., 2005) and for the pertuzumab and trastuzumab complexes with the extracellular region ErbB2 (Cho et al., 2003; Franklin et al., 2004) are all somewhat higher, in the range from 0.70 to 0.75, perhaps reflecting the more convex shape of the matuzumab epitope compared to those of these other antibody drugs.

Neither the conformation of sEGFRd3 nor that of Fab72000 is significantly altered upon formation of the complex. There are very minor differences in the side chain positions in both the domain III epitope and in the CDRs of the Fab. Most notably, Y103 in the V_H domain is disordered in the unbound Fab and becomes ordered on interacting with sEGFR. The elbow angle changes by only 4° between the bound and unbound Fab72000, which is in within the range expected due to dynamic elbow flexibility (Stanfield et al., 2006).

Not only is the conformation of domain III unaltered by Fab72000 binding, but also the location of the bound Fab72000 would not be expected to disrupt the tethered configuration of sEGFR (Figure 1, left panel), the preferred solution conformation of the receptor (Dawson et al., 2007), and the likely conformation of the unliganded receptor at the cell surface. Fab72000 can readily be docked onto its epitope on either of the two known structures of tethered sEGFR (PDB IDs 1NQL and 1YY9) without hindrance from any of the other domains of sEGFR.

The Matuzumab Epitope Is Distinct from the Ligand-Binding Site on Domain III of sEGFR

To confirm that the crystallographically defined epitope for matuzumab precisely represents what is seen in solution, we generated site-specific alterations in sEGFR at key amino acids in the domain III matuzumab epitope (Figures 3B and 4A). Each alteration was introduced in the context of the full-length extracellular domain and these altered sEGFR proteins expressed and purified using appropriately baculovirus infected Sf9 cells. Each purified, altered sEGFR was analyzed for binding to immobilized Fab72000 and to immobilized EGF, exactly as described (Li et al., 2005). Alteration to alanine of either of the two lysines on the epitope loop (K454A or K463A) leads to an approximate 100-fold reduction in the affinity of sEGFR for Fab72000 (Figure 4B). Substitution of alanines at T459 and S460 (T459A/T460A) also dramatically reduces the binding affinity. The combination of either lysine to alanine substitution with T459A/T460A abolishes all detectable interaction between sEGFR and the immobilized Fab72000.

As shown in Figure 4A, the binding sites for matuzumab and for EGF on domain III do not overlap. As would be predicted based upon this observation, the sEGFR proteins with alterations in the Fab72000 epitope bind to immobilized EGF with near wild-type affinity (Figure 4B). This also confirms that the striking reduction in binding affinity of these altered sEGFR proteins for Fab72000 is not due to a global disruption of the structure of domain III of sEGFR. Finally, substitution of two amino acids that are known to be critical for EGF binding (D355T/F357A) have negligible effect on binding of sEGFR to Fab72000.

Not only is there no overlap of the epitope for matuzumab and the ligand binding region on domain III, but a bound Fab72000 would impose no steric hindrance to the binding of EGF or of

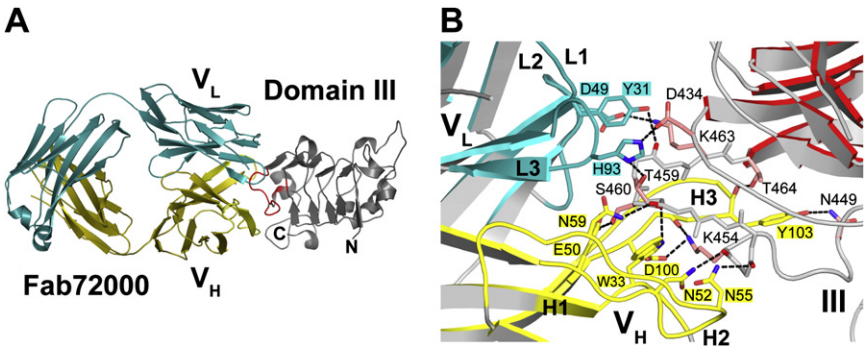

Figure 3. Structure of the Complex between the Matuzumab Fab Fragment and Domain III of sEGFR

(A) Cartoon of the Fab72000/sEGFRd3 complex. Domain III is colored in gray with the epitope highlighted in red. The orientation of domain III is the same as for the tethered sEGFR (left-hand view) in Figure 1. Fab72000 is colored cyan for the light chain and yellow for the heavy chain.

(B) A closeup view of the interactions between Fab72000 and domain III of sEGFR. Domain III is in gray with the secondary structure elements highlighted in red. The V_L and V_H domains of Fab72000 are in gray with cyan and yellow highlights, respectively. The CDRs of Fab72000 are shown in cyan for L1, L2, and L3 of the V_L domain, and in yellow for H1, H2, and H3 of the V_H domain. The side chains of the amino acids participating in key interactions are shown, colored as for the CDRs for the Fab and in pink for domain III. The amino acids are labeled on a cyan background for those from V_L, on a yellow background for V_H, and in black for sEGFRd3. Distances consistent with hydrogen bonds are shown with dashed black lines.

TGFα to domain III. With domain III from the Fab72000/sEGFRd3 complex overlaid on domain III from the sEGFR/EGF complex (PDB ID 1IVO) the closest approach of the Fab and EGF is 9 Å. This is in stark contrast to the situation for cetuximab binding. There is a high degree of overlap between the cetuximab and EGF-binding sites on domain III (Figure 4C). The steric block of this ligand-binding site is the primary mechanism of cetuximab-mediated inhibition of ligand-induced dimerization and activation of EGFR (Li et al., 2005). Clearly the mechanism of inhibition of EGFR activation by matuzumab must be different.

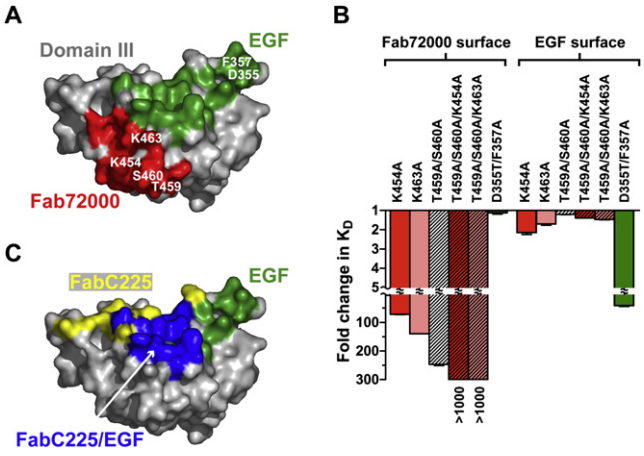

Figure 4. The Matuzumab Epitope Is Distinct from the Ligand-Binding Site on Domain III

(A) A surface representation of domain III is shown in gray viewed in approximately the same orientation as in Figure 3. Amino acids on domain III that are within 4 Å of Fab72000 (red) or of EGF (green) are indicated on this surface. The amino acids that were altered (see [B]) are labeled in white.

(B) Surface Plasmon Resonance (SPR) analysis of the binding of altered sEGFR proteins to immobilized Fab72000 or EGF. The equilibrium binding K_D values for each protein were determined exactly as described in the legend to Figure 2A. The fold change in this K_D value for each altered protein relative to that for the binding of wild-type sEGFR to each immobilized ligand is plotted. Error bars indicate the standard deviation on at least three independent sets of measurements.

(C) The same surface representation of domain III as in (A) is shown with the contacting amino acids for FabC225 in yellow, for EGF in green, and for the region of overlap between FabC225 and EGF in blue.

Implications for the Mechanism of Inhibition of EGFR Activation by Matuzumab

If matuzumab does not directly block access of the ligand to the domain III ligand-binding site, how does it prevent high-affinity ligand binding, receptor dimerization, and activation? To understand this, we consider the effect of the binding of Fab72000 upon the formation of the ligand-induced dimeric form of the receptor. As shown in Figure 1, sEGFR undergoes a dramatic domain rearrangement in going from the tethered inactive state to the ligand-bound dimeric state (Burgess et al., 2003). Additional local structural changes in domain II are known to be key for high-affinity ligand binding, receptor dimerization, and activation (Dawson et al., 2005; Ogiso et al., 2002). As shown in Figure 5, and discussed in detail below, when domain III from the Fab72000/sEGFRd3 complex is overlaid on domain III from the receptor in its extended, dimerization-competent conformation (PDB ID 1MOX), there are direct clashes between the bound Fab72000 and both domains I and II of the extended receptor. With matuzumab bound to domain III of EGFR, the receptor cannot undergo the large-scale domain rearrangement that is required for dimerization. Further, the binding of Fab72000 blocks the critical local conformational changes in domain II.

With the receptor in the extended conformation, the N-terminal region of the domain I clashes with the light chain of Fab72000, preventing domain I from reaching the position that is required for high-affinity ligand binding (indicated with an arrow in Figure 5A). This is reminiscent in nature and extent to clashes between the antigen-binding fragment of cetuximab (FabC225) and domain I that were previously implicated as part of the mechanism of inhibition of EGFR dimerization by that antibody (Li et al., 2005). In that case, the different orientation of FabC225 on domain III positions the V_H domain such as to occlude the N-terminal portion of domain I from its required position in the receptor dimer.

Clashes between domain II of the extended receptor and the Fab were not seen in the cetuximab complex, and are significant. With Fab72000 bound to domain III of EGFR, it would not be possible for the C-terminal portion of domain II to adopt the conformation observed in the ligand-bound dimeric form of the receptor. As shown in Figure 5B, if Fab72000 is docked onto its epitope on domain III of an sEGFR molecule in the extended conformation, there are clashes along the C-terminal half of

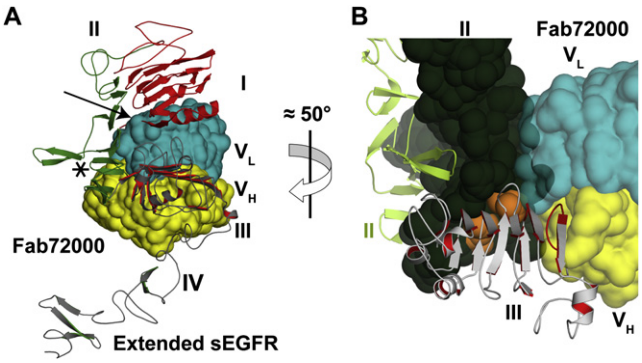

Figure 5. Implications for the Mechanism of Inhibition of EGFR by Matuzumab

(A) Cartoon of the extended sEGFR with Fab72000, in surface representation, docked onto its domain III epitope. The orientation of the receptor is the same as for the right-hand protomer in the sEGFR dimer shown in Figure 1 (with domains colored as for the left-hand protomer; EGF is omitted for clarity). The Fab72000 is colored as in Figure 3. The N-terminal region of domain I clashes with the V_L domain (indicated with an arrow). Additional clashes occur along the C-terminal half of domain II (see [B]). The C-terminal loop on domain II (D278, H280) that makes critical contacts across the dimer interface is marked with an asterisk.

(B) In this view, an approximate 50° rotation about the vertical axis relative to (A), domain II is shown in sphere representation in dark green. A cartoon of domain II of the other molecule in the dimer is shown (light green) for reference. Domain I has been omitted for clarity. The V_L domain of the Fab clashes with domain II in the critical C-terminal region that forms the binding pocket for the dimerization arm and makes important contacts with domain III (from N274 and E293 in domain II, colored orange). These interactions are known to be crucial for stabilizing the dimerization competent conformation of domain II. The Fab72000 epitope loop on domain III is colored in red.

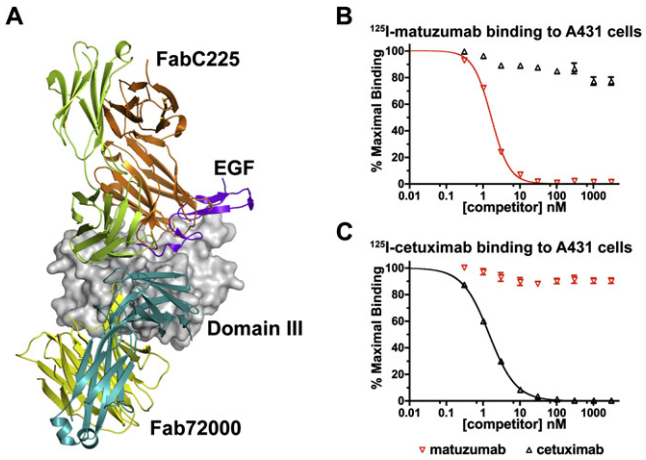

Figure 6. The Matuzumab and Cetuximab Epitopes Do Not Overlap

(A) A surface representation of the domain III as in Figure 4 is shown. Cartoons of Fab72000, FabC225 (PDB ID 1YY9), and EGF (PDB ID 1IVO) are shown docked onto their respective binding sites on domain III. Fab72000 is colored as in Figure 3A, FabC225 is shown with the heavy chain in orange and the light chain in light green, and EGF is in purple.

(B and C) Competition of matuzumab (red triangles) or cetuximab (black triangles) for binding of ^{125}I-labeled matuzumab (B) or ^{125}I-labeled cetuximab (C) to A431 cells, performed and analyzed as described in Figure 2B.

domain II, predominantly with the V_L domain of the Fab. This C-terminal half of domain II forms the binding pocket for the dimerization arm from the other molecule in the receptor dimer. Additional interactions across the dimer interface from a C-terminal loop on domain II (D279 and H280, marked with an asterisk in Figure 5A) contribute substantially to the stability of the EGFR dimer. The conformation of domain II in this region is stabilized by interactions with domain III that have been demonstrated to be critical for EGFR dimerization and activation (Dawson et al., 2005; Ogiso et al., 2002). The binding of Fab72000 to domain III would disrupt all of these interactions. Thus, Fab72000 binding to domain III of EGFR blocks the global domain rearrangement of EGFR and the local conformational changes in domain II. We propose that blocking both of these key elements in formation of the productive EGFR dimer is critical for the effective inhibition of EGFR activation by matuzumab.

The steric restriction on EGFR conformation imposed by the binding of matuzumab offers a structural framework to explain the competition data presented in Figure 2. When matuzumab (or just its antigen-binding domain, Fab72000) binds to the extracellular region of EGFR, the receptor cannot adopt the conformation required for both domains I and III to engage in ligand binding. However, the ligand-binding site on domain III is completely exposed. EGF can bind to this site with low affinity (approximately 1 μM; Kohda et al., 1993; Lemmon et al., 1997; Li et al., 2005). Under the conditions of the cell-based assay, weak binding of EGF to only domain III of EGFR is not detected. By preventing the receptor from adopting the conformation required for the bipartite binding of EGF between domains I and III, matuzumab blocks all detectable binding of EGF to cell surface EGFR in this assay. By contrast, the Biacore assay is performed at a much higher concentration of soluble ligand (in this case 600 nM sEGFR, which binds to immobilized EGF). Under these conditions, the monovalent binding of domain III alone to EGF can be detected. In the Biacore assay, the residual binding to immobilized EGF observed for sEGFR in the presence of excess Fab72000 is due, at least in part, to binding to EGF of the exposed domain III in an Fab72000/sEGFR complex.

Implications for the Therapeutic Application of Matuzumab

As discussed above, the mechanism of inhibition of matuzumab is different from that previously described for cetuximab. Both antibodies effectively block productive binding of EGF to cell surface EGFR (Figure 2B) but do so by interacting with distinct epitopes on domain III. Not only are the epitopes nonoverlapping, but the structures suggest that both antibodies could simultaneously bind to EGFR. As shown in Figure 6A, when FabC225 and Fab72000 are simultaneously docked onto their respective epitopes on domain III the two Fab fragments occupy different positions and do not clash. This observation is consistent with cellular competition assays. Excess cetuximab is unable to compete with the binding of ^{125}I-labeled matuzumab to the cell surface EGFR on A431 cells (Figure 6B). Similarly matuzumab cannot compete for ^{125}I-labeled cetuximab binding (Figure 6C). Further, it has been reported that there are an increased number of cell surface antibody-binding sites for a mixture of matuzumab and cetuximab compared to either antibody alone (Kreysch and Schmidt, 2004). This suggests that both matuzumab and cetuximab can bind to a single receptor molecule at the cell surface.

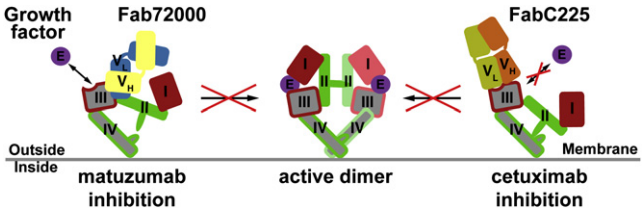

Figure 7. Matuzumab and Cetuximab Use Different Mechanisms to Block Ligand-Induced EGFR Dimerization and Activation

In the center of the scheme, the ligand-induced sEGFR dimer is represented, with domain I in red, domain II in green, domain III in gray with red border, domain IV in gray with green border, and the ligand (E) in violet. The colors for one protomer are lightened for contrast. On the left-hand side a scheme is shown to illustrate the mechanism of inhibition of ligand-induced dimerization by matuzumab. Fab72000 binds to domain III of sEGFR and sterically prevents the receptor from adopting the conformation required for dimerization. Importantly, Fab72000 blocks the local conformational changes in domain II that are critical for both high-affinity ligand binding and dimerization. The inhibition is noncompetitive; the ligand-binding site on domain III is not blocked. This contrasts with the mechanism of inhibition previously reported for cetuximab (Li et al., 2005). FabC225 (right side) is a competitive inhibitor that blocks the ligand-binding site on domain III. This is the primary mechanism of inhibition of ligand-mediated dimerization by cetuximab.

Treatment of cells with combinations of antibodies against distinct epitopes on the extracellular domain of EGFR, and on the related family member ErbB2, leads to enhanced receptor internalization and degradation (Friedman et al., 2005), a factor that contributes to the antitumor activity of many therapeutic antibodies. Matuzumab and cetuximab can both bind simultaneously to EGFR, and this has the potential to lead to synergistic antitumor effects. Combination of matuzumab and cetuximab could thus be beneficial in cancer therapy.

Conclusion

EGFR dimerization requires a conformational reorganization of the receptor extracellular region that is promoted by ligand binding to domains I and III (Figures 1 and 7). As shown schematically in Figure 7, cetuximab acts as a competitive inhibitor, preventing ligand-induced dimerization by directly blocking access of ligand to the domain III ligand-binding site. By contrast, matuzumab does not occlude the ligand-binding site on domain III. Rather, matuzumab exploits a noncompetitive mechanism to inhibit sEGFR dimerization and activation. Inhibition of ligand-induced EGFR activation by matuzumab is entirely dependent on sterically blocking the receptor from adopting the conformation that is required for high-affinity ligand binding and dimerization. These different mechanisms of inhibition suggest opportunities to exploit multiple EGFR-targeting drugs to act synergistically for optimal therapeutic gain.

EXPERIMENTAL PROCEDURES

Protein Expression and Purification

sEGFR and sEGFRd3 were expressed in baculovirus-infected Sf9 cells, purified as described (Ferguson et al., 2000; Li et al., 2005) and used without modification of their glycosylation state. Matuzumab (EMD72000) was provided by Merck KGaA. The Fab fragment of matuzumab (Fab72000) was generated by papain cleavage using the ImmunoPure Fab Preparation Kit (Pierce) and used without additional purification. Fab72000/sEGFR complex was generated exactly as described (Li et al., 2005). To generate the complex with sEGFRd3, Fab was mixed with a 1.2-fold molar excess of sEGFRd3 and excess sEGFRd3 separated from Fab72000/sEGFRd3 complex by SEC using a Bio-Silect SEC250 column (Bio-Rad), equilibrated with 20 mM HEPES and 100 mM NaCl (pH 7.5).

Crystallization and Data Collection

Proteins were concentrated and buffer exchanged into 10 mM HEPES and 50 mM NaCl (pH 7.5) and crystallized using the hanging drop vapor diffusion method. Large single crystals of Fab72000 were obtained by mixing equal volumes (1 μl) of the Fab (13 mg/ml) with a solution containing 1.8 M ammonium sulfate and 0.1 M MES (pH 6.5) and equilibrating over a reservoir of this buffer at 20°C. Crystals were flash frozen in reservoir solution that was supplemented with 9% sucrose, 2% glucose, 8% glycerol, and 8% ethylene glycol. X-ray diffraction data were collected at the Cornell High Energy Synchrotron Source (CHESS) beamline F1, using an ADSC Quantum-210 CCD detector. Fab72000/sEGFRd3 was crystallized by mixing equal parts (1 μl) of the SEC purified complex (14 mg/ml) with 1 M NaCl, 16% PEG 3350, and 50 mM MES (pH 6.0) and equilibrating over a reservoir of the same buffer at 20°C. Streak seeding was used to produce large single crystals (0.5 × 0.1 × 0.15 mm) that were cryostabilized by serial transfer to solutions of reservoir containing increasing concentrations of ethylene glycol. Following transfer to the final cryostabilizer of reservoir plus 15% ethylene glycol, crystals were flash frozen in liquid nitrogen. Data were collected at the Swiss Light Source (SLS) beamline X06SA, using a Mar225 CCD detector. All data were processed in HKL2000 (Otwinowski and Minor, 1997). Data collection statistics are summarized in Table 1.

Structure Determination and Refinement

The structures of the Fab72000 and Fab72000/sEGFRd3 were solved by the method of MR using the program PHASER (CCP4, 1994). To solve the Fab structure, the coordinates for Fab2C4 (PDB ID 1L7I) (Vajdos et al., 2002) were selected as the initial search model based on the sequence identity between Fab2C4 and Fab72000. To solve the Fab72000/sEGFRd3 structure, one of the two Fab fragments in the asymmetric unit was first located using the refined Fab72000 coordinates as search model. With the position of this Fab fragment fixed, a second search using the coordinates of domain III of sEGFR (amino acids 310–500 from PDB ID 1YY9) located one of the sEGFRd3 molecules. Subsequently, the second Fab72000/sEGFRd3 complex in the asymmetric unit was found. Coordinates were manually rebuilt in COOT (Emsley and Cowtan, 2004) and refined using CNS (Brünger et al., 1998) and Refmac (CCP4, 1994). New maps were calculated following each iteration of refinement, including solvent flattened maps with minimized model bias calculated using the program DM (CCP4, 1994). Refinement statistics are summarized in Table 1.

SPR/Biacore-Binding Studies

Surface Plasmon Resonance (SPR)/Biacore studies were carried out using a Biacore 3000 instrument at 25°C in 10 mM Tris, 150 mM NaCl, 3 mM EDTA, and 0.005% Tween-20 (pH 8.0). Fab72000 was immobilized on a Biacore CM5 biosensor chip as follows: the CM-dextran matrix was activated with *N*-ethyl-*N*′-(dimethylaminopropyl)-carbodiimide hydrochloride (EDC) and *N*-hydroxysuccinimide (NHS). Fab72000 (500 ng) was flowed over this activated surface at a concentration of 5 μg/ml in 10 mM sodium acetate (pH 5.0) at 5 μl per minute for 20 min. The remaining reactive sites were blocked with 1 M ethanolamine-HCl (pH 8.5). Immobilized Fab fragment contributed a signal of 1436 response units (RU). The surface was regenerated between sEGFR injections with two 5 μl injections of 10 mM glycine and 1 M NaCl (pH 2.5) to remove remaining bound sEGFR. EGF immobilization and sEGFR-binding analysis were performed exactly as described (Ferguson et al., 2000). Data were analyzed using Prism 4 (GraphPad Software, Inc.).

Cell-Based Binding Studies

^{125}I-labeled EGF, matuzumab, and cetuximab were generated with specific activities of 1750 Ci/mmol, 273 Ci/mmol, and 238 Ci/mmol, respectively. A431 epidermoid carcinoma cells were plated in 96-well dishes and grown to 75%–90% confluence. Cells were washed twice with ice-cold DMEM containing 1% BSA (incubation medium) and incubated in this medium containing 3 nM radiolabeled ligand plus the relevant cold competitor (200 μl/well) for 6 hr at 4°C. Cells were washed three times with ice-cold incubation medium and were lysed with

1 M NaOH (200 μl/well). The wells were washed with 200 μl of water, and liquid scintillation counting was used to determine the counts of bound ^{125}I-labeled species. Data were analyzed using Prism 4 (GraphPad Software, Inc.).

Generation of sEGFR Epitope Mutations

Standard PCR-directed site-directed mutagenesis strategies were used to produce the appropriate DNA in the pFastBac vector. The following mutations were made: K454A, K463A, T459A/S460A, K454A/T459A/S460A, and T459A/S460A/K463A. The generation of recombinant baculovirus, overexpression in Sf9 cells, and protein purification were exactly as described before for wild-type sEGFR (Ferguson et al., 2000).

ACCESSION NUMBERS

Coordinates of the Fab72000 and Fab72000/sEGFRd3 structures have been deposited, with PDB ID codes 3C08 and 3C09, respectively.

SUPPLEMENTAL DATA

The Supplemental Data include one supplemental figure and can be found with this article online at http://www.cancercell.org/cgi/content/full/13/4/365/DC1/.

ACKNOWLEDGMENTS

We thank Karl Schmitz, Steve Stayrook, Per Hillertz, and Djordje Musil for assistance with data collection; Jens Oliver Funk for support of this collaboration; Volker Doetsch (Johann Wolfgang Goethe Universität, Frankfurt, Germany) for assuming the role of dissertation supervisor to J.S.; Christof Reusch and Juergen Schmidt for performing the radiolabeled binding experiments; and Mark Lemmon and members of the Ferguson and Lemmon laboratories at the University of Pennsylvania for valuable discussions and critical comments on the manuscript. J.S. conducted all other experiments in the laboratory of K.M.F., under direct daily detailed guidance from K.M.F. and valuable periodic supervision of T.K. J.S. solved the structures described in this manuscript at the University of Pennsylvania, with assistance from S.L., Karl Schmitz, and K.M.F. T.K. established the University of Pennsylvania /Merck KGaA collaboration and provided scientific advice to J.S. The research of K.M.F. is supported by a Career Award in the Biomedical Sciences from the Burroughs Wellcome Fund, and by NIH grant R01-CA112552. K.M.F. is also the Dennis and Marsha Dammerman Scholar supported by the Damon Runyon Cancer Research Foundation (DRS-52-06). This work is based upon research conducted at (1) the Cornell High Energy Synchrotron Source (CHESS), which is supported by the National Science Foundation under award DMR 97-13424, using the Macromolecular Diffraction at CHESS (MacCHESS) facility, which is supported by award RR-01646 from the National Institutes of Health, through its National Center for Research Resources, and (2) the Swiss Light Source (SLS), Villigen. The Biacore instrument utilized in this study was funded by grants from the NIH and the University of Pennsylvania to the Ferguson and Lemmon laboratories. T.K. and A.B. are employees of Merck KGaA, the manufacturer of the drug matuzumab. J.S. is a Ph.D. student at Merck KGaA under supervision of T.K. J.S. conducted this work as a Visiting Research Scholar in the laboratory of K.M.F. at the University of Pennsylvania. This collaboration is governed by a Supported Research Agreement between Merck KGaA and the Trustees of the University of Pennsylvania and is financially supported in part by Merck KGaA.

Received: November 19, 2007
Revised: January 21, 2008
Accepted: February 27, 2008
Published: April 7, 2008

REFERENCES

Bier, H., Hoffmann, T., Hauser, U., Wink, M., Ochler, M., Kovar, A., Müser, M., and Knecht, R. (2001). Clinical trial with escalating doses of the antiepidermal growth factor receptor humanized monoclonal antibody EMD 72 000 in patients with advanced squamous cell carcinoma of the larynx and hypopharynx. Cancer Chemother. Pharmacol. *47*, 519–524.

Bouyain, S., Longo, P.A., Li, S., Ferguson, K.M., and Leahy, D.J. (2005). The extracellular region of ErbB4 adopts a tethered conformation in the absence of ligand. Proc. Natl. Acad. Sci. USA *102*, 15024–15029.

Brünger, A.T., Adams, P.D., Clore, G.M., DeLano, W.L., Gros, P., Grosse-Kunstleve, R.W., Jiang, J.S., Kuszewski, J., Nilges, M., Pannu, N.S., et al. (1998). Crystallography & NMR system: A new software suite for macromolecular structure determination. Acta Crystallogr. *D54*, 905–921.

Burgess, A.W., Cho, H.S., Eigenbrot, C., Ferguson, K.M., Garrett, T.P.J., Leahy, D.J., Lemmon, M.A., Sliwkowski, M.X., Ward, C.W., and Yokoyama, S. (2003). An open-and-shut case? Recent insights into the activation of EGF/ErbB receptors. Mol. Cell *12*, 541–552.

CCP4 (Collaborative Computational Project, Number 4). (1994). The CCP4 suite: Programs for protein crystallography. Acta Crystallogr. D Biol. Crystallogr. *50*, 760–763.

Cho, H.S., and Leahy, D.J. (2002). Structure of the extracellular region of HER3 reveals an interdomain tether. Science *297*, 1330–1333.

Cho, H.S., Mason, K., Ramyar, K.X., Stanley, A.M., Gabelli, S.B., Denney, D.W., and Leahy, D.J. (2003). Structure of the extracellular region of HER2 alone and in complex with the Herceptin Fab. Nature *421*, 756–760.

Dawson, J.P., Berger, M.B., Lin, C.C., Schlessinger, J., Lemmon, M.A., and Ferguson, K.M. (2005). Epidermal growth factor receptor dimerization and activation require ligand-induced conformational changes in the dimer interface. Mol. Cell. Biol. *25*, 7734–7742.

Dawson, J.P., Bu, Z., and Lemmon, M.A. (2007). Ligand-induced structural transitions in ErbB receptor extracellular domains. Structure *15*, 942–954.

Emsley, P., and Cowtan, K. (2004). Coot: Model-building tools for molecular graphics. Acta Crystallogr. *D60*, 2126–2132.

Ferguson, K.M. (2004). Active and inactive conformations of the epidermal growth factor receptor. Biochem. Soc. Trans. *32*, 742–745.

Ferguson, K.M., Darling, P.J., Mohan, M.J., Macatee, T.L., and Lemmon, M.A. (2000). Extracellular domains drive homo- but not hetero-dimerization of ErbB receptors. EMBO J. *19*, 4632–4643.

Ferguson, K.M., Berger, M.B., Mendrola, J.M., Cho, H.S., Leahy, D.J., and Lemmon, M.A. (2003). EGF activates its receptor by removing interactions that autoinhibit ectodomain dimerization. Mol. Cell *11*, 507–517.

Franklin, M.C., Carey, K.D., Vajdos, F.F., Leahy, D.J., de Vos, A.M., and Sliwkowski, M.X. (2004). Insights into ErbB signaling from the structure of the ErbB2-pertuzumab complex. Cancer Cell *5*, 317–328.

Friedman, L.M., Rinon, A., Schechter, B., Lyass, L., Lavi, S., Bacus, S.S., Sela, M., and Yarden, Y. (2005). Synergistic down-regulation of receptor tyrosine kinases by combinations of mAbs: Implications for cancer immunotherapy. Proc. Natl. Acad. Sci. USA *102*, 1915–1920.

Garrett, T.P.J., McKern, N.M., Lou, M., Elleman, T.C., Adams, T.E., Lovrecz, G.O., Zhu, H.J., Walker, F., Frenkel, M.J., Hoyne, P.A., et al. (2002). Crystal structure of a truncated epidermal growth factor receptor extracellular domain bound to transforming growth factor alpha. Cell *110*, 763–773.

Graeven, U., Kremer, B., Südhoff, T., Killing, B., Rojo, F., Weber, D., Tillner, J., Unal, C., and Schmiegel, W. (2006). Phase I study of the humanised anti-EGFR monoclonal antibody matuzumab (EMD 72000) combined with gemcitabine in advanced pancreatic cancer. Br. J. Cancer *94*, 1293–1299.

Hubbard, S.R., and Miller, W.T. (2007). Receptor tyrosine kinases: Mechanisms of activation and signaling. Curr. Opin. Cell Biol. *19*, 117–123.

Johns, T.G., Adams, T.E., Cochran, J.R., Hall, N.E., Hoyne, P.A., Olsen, M.J., Kim, Y.S., Rothacker, J., Nice, E.C., Walker, F., et al. (2004). Identification of the epitope for the epidermal growth factor receptor-specific monoclonal antibody 806 reveals that it preferentially recognizes an untethered form of the receptor. J. Biol. Chem. *279*, 30375–30384.

Kettleborough, C.A., Saldanha, J., Heath, V.J., Morrison, C.J., and Bendig, M.M. (1991). Humanization of a mouse monoclonal antibody by CDR-grafting: The importance of framework residues on loop conformation. Protein Eng. *4*, 773–783.

Kohda, D., Odaka, M., Lax, I., Kawasaki, H., Suzuki, K., Ullrich, A., Schlessinger, J., and Inagaki, F. (1993). A 40-kDa epidermal growth factor/transforming growth factor alpha-binding domain produced by limited proteolysis of the

extracellular domain of the epidermal growth factor receptor. J. Biol. Chem. *268*, 1976–1981.

Kreysch, H.G., and Schmidt, J. (2004). Pharmaceutical compositions directed to Erb-B1 receptors. Merck Patent GMBH (DE), EP1549344. April 2004. WO 2004/032960 A1.

Kollmannsberger, C., Schittenhelm, M., Honecker, F., Tillner, J., Weber, D., Oechsle, K., Kanz, L., and Bokemeyer, C. (2006). A phase I study of the humanized monoclonal anti-epidermal growth factor receptor (EGFR) antibody EMD 72000 (matuzumab) in combination with paclitaxel in patients with EGFR-positive advanced non-small-cell lung cancer (NSCLC). Ann. Oncol. *17*, 1007–1013.

Lawrence, M.C., and Colman, P.M. (1993). Shape complementarity at protein/protein interfaces. J. Mol. Biol. *234*, 946–950.

Lemmon, M.A., Bu, Z., Ladbury, J.E., Zhou, M., Pinchasi, D., Lax, I., Engelman, D.M., and Schlessinger, J. (1997). Two EGF molecules contribute additively to stabilization of the EGFR dimer. EMBO J. *16*, 281–294.

Li, S., Schmitz, K.R., Jeffrey, P.D., Wiltzius, J.J.W., Kussie, P., and Ferguson, K.M. (2005). Structural basis for inhibition of the epidermal growth factor receptor by cetuximab. Cancer Cell *7*, 301–311.

Mendelsohn, J., and Baselga, J. (2006). Epidermal growth factor receptor targeting in cancer. Semin. Oncol. *33*, 369–385.

Molina, M.A., Codony-Servat, J., Albanell, J., Rojo, F., Arribas, J., and Baselga, J. (2001). Trastuzumab (herceptin), a humanized anti-Her2 receptor monoclonal antibody, inhibits basal and activated Her2 ectodomain cleavage in breast cancer cells. Cancer Res. *61*, 4744–4749.

Murthy, U., Basu, A., Rodeck, U., Herlyn, M., Ross, A.H., and Das, M. (1987). Binding of an antagonistic monoclonal antibody to an intact and fragmented EGF-receptor polypeptide. Arch. Biochem. Biophys. *252*, 549–560.

Ogiso, H., Ishitani, R., Nureki, O., Fukai, S., Yamanaka, M., Kim, J.H., Saito, K., Sakamoto, A., Inoue, M., Shirouzu, M., et al. (2002). Crystal structure of the complex of human epidermal growth factor and receptor extracellular domains. Cell *110*, 775–787.

Otwinowski, Z., and Minor, W. (1997). Processing of X-ray diffraction data collected in oscillation mode. In Macromolecular Crystallography, *Volume 276*, C.W. Carter and R.M. Sweet, eds. (New York: Academic Press), pp. 307–326.

Rodeck, U., Herlyn, M., Herlyn, D., Molthoff, C., Atkinson, B., Varello, M., Steplewski, Z., and Koprowski, H. (1987). Tumor growth modulation by a monoclonal antibody to the epidermal growth factor receptor: Immunologically mediated and effector cell-independent effects. Cancer Res. *47*, 3692–3696.

Rodeck, U., Williams, N., Murthy, U., and Herlyn, M. (1990). Monoclonal antibody 425 inhibits growth stimulation of carcinoma cells by exogenous EGF and tumor-derived EGF/TGF-alpha. J. Cell Biol. *44*, 69–79.

Schlessinger, J. (2000). Cell signaling by receptor tyrosine kinases. Cell *103*, 211–225.

Seiden, M.V., Burris, H.A., Matulonis, U., Hall, J.B., Armstrong, D.K., Speyer, J., Weber, J.D.A., and Muggia, F. (2007). A phase II trial of EMD72000 (matuzumab), a humanized anti-EGFR monoclonal antibody, in patients with platinum-resistant ovarian and primary peritoneal malignancies. Gynecol. Oncol. *104*, 727–731.

Socinski, M.A. (2007). Antibodies to the epidermal growth factor receptor in non small cell lung cancer: Current status of matuzumab and panitumumab. Clin. Cancer Res. *13*, 4597–4601.

Stanfield, R.L., Zemla, A., Wilson, I.A., and Rupp, B. (2006). Antibody elbow angles are influenced by their light chain class. J. Mol. Biol. *31*, 1566–1574.

Sundberg, E.J., and Mariuzza, R.A. (2002). Molecular recognition in antibody-antigen complexes. Adv. Protein Chem. *61*, 119–160.

Vajdos, F.F., Adams, C.W., Breece, T.N., Presta, L.G., de Vos, A.M., and Sidhu, S.S. (2002). Comprehensive functional maps of the antigen-binding site of an anti-ErbB2 antibody obtained with shotgun scanning mutagenesis. J. Mol. Biol. *320*, 415–428.

Vanhoefer, U., Tewes, M., Rojo, F., Dirsch, O., Schleucher, N., Rosen, O., Tillner, J., Kovar, A., Braun, A.H., Trarbach, T., et al. (2004). Phase I study of the humanized antiepidermal growth factor receptor monoclonal antibody EMD72000 in patients with advanced solid tumors that express the epidermal growth factor receptor. J. Clin. Oncol. *22*, 175–184.

Zhang, X., Gureasko, J., Shen, K., Cole, P.A., and Kuriyan, J. (2006). An allosteric mechanism for activation of the kinase domain of epidermal growth factor receptor. Cell *125*, 1137–1149.